

Room-temperature ultra-sensitive mass spectrometer via dynamic decoupling

Nan Zhao^{1,*} and Zhang-qi Yin²

¹Beijing Computational Science Research Center, Beijing 100084, China

²The Center for Quantum Information, Institute for Interdisciplinary Information Sciences, Tsinghua University, Beijing 100084, P. R. China

We propose an ultra-sensitive mass spectrometer based on a coupled quantum-bit-oscillator system. Under dynamical decoupling control of the quantum bit (qubit), the qubit coherence exhibits a comb structure in time domain. The time-comb structure enables high precision measurement of oscillator frequency, which can be used as an ultra-sensitive mass spectrometer. Surprisingly, in ideal case, the sensitivity of the proposed mass spectrometer, which scales with the temperature T as $T^{-1/2}$, has better performance in higher temperature. While taking into account qubit and oscillator decay, we show that the optimal sensitivity is independent on environmental temperature T . With present technology on solid state spin qubit and high-quality optomechanical system, our proposal is feasible to realize an ultra-sensitive mass spectrometer in room temperature.

Introduction- Single quantum objects, such as single atoms and single photons, attracted more and more attentions in recent years. Novel applications, such as quantum information processing, triggered fast technique development in *isolating* single quantum objects from the noisy environment, precisely *controlling* their quantum states, and *hybridizing* different quantum systems. The technique development, in turn, provides opportunities of using single quantum objects to design more distinctive and more powerful tools in various research fields.

Detection of extremely weak signals, such as magnetic fields produced by single nuclei [1–5], and tiny mass of single molecules [6–10], has broad applications in chemistry and biology. In the past a few decades, detectors based on single quantum objects were designed, and their sensitivity was progressively improved. For example, using mechanical cantilevers or well-controlled single spins, people are able to detect and resolve single spins of electrons [11] and nuclei [1–3]. For mass sensors, the minimum detectable mass was decreased from femtogram to yoctogram [7–10], reaching the single-proton limit.

In this Letter, we propose an ultra-sensitive measurement scheme based on a coupled quantum-bit-oscillator system. We show that, with many-pulse dynamical decoupling (DD) control [12] on the quantum bit (qubit) of the coupled system, the qubit coherence exhibits periodic sharp peaks, forming a *comb structure* in time domain. The qubit coherence peaks are synchronized with the oscillator period, and the peak width decreases when increasing the measurement resource, namely, the DD control pulse number. With this time-comb structure of the qubit coherence, tiny changes of the oscillator frequency, e.g., due to absorption of a single molecule onto a mechanical oscillator, can be monitored and precisely determined from the shift of the coherence peaks.

Two distinctive features make our proposal possible to reach ultra-high sensitivity and have outstanding performance in room temperature. Firstly, the measurement sensitivity scales with the control pulse number N as $\sim N^{-3/2}$, which is different in comparison to $N^{-1/2}$ -dependence in the magnetometry schemes using single qubit [13]. The improved scaling relation enables us reach high sensitivity faster, with less

measurement resource. Secondly, we show that the optimal sensitivity is *independent* on environmental temperature T . Furthermore, in high temperature, less control pulses are required to reach the optimal sensitivity and the proposed mass spectrometer has better performance. For most of the conventional sensing schemes, low-temperature (e.g., liquid Helium temperature) is required, since measurement sensitivity is usually limited by thermal fluctuation which is proportional to $\sqrt{k_B T}$ (with Boltzmann constant k_B) [14]. The temperature-independent feature of the optimal sensitivity in our proposal allows novel applications in room temperature,

Recent technique development on solid-state qubit and mechanical oscillator provides the feasibility of our proposal. Solid-state single spin qubit, such as nitrogen-vacancy (NV) centers [15, 16], has been demonstrated to be well isolated with long coherence time [17]. Meanwhile, the mechanical oscillators of micro- or nano-size have been experimentally fabricated and widely used in detecting weak signals [14, 18]. Particularly, the recent optomechanical systems [6, 19, 20], optically levitated particles [21–24], are believed to reach high

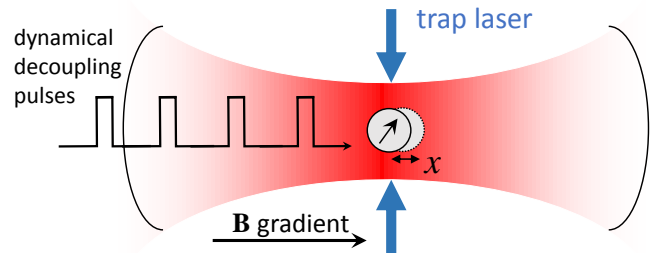


FIG. 1. (Color online) Schematic of the proposed mass spectrometer. A nano-diamond is trapped in a harmonic potential by counter-propagating laser. The nano-diamond (the grey circle) contains an NV center, which serves as a qubit. With a gradient magnetic field, the center-of-mass motion of the nano-diamond couples to the NV center spin. Under DD control, the qubit coherence exhibits time-comb structure, which can be used to measure the tiny change of the oscillation frequency (thus the mass change) of the nano-diamond.

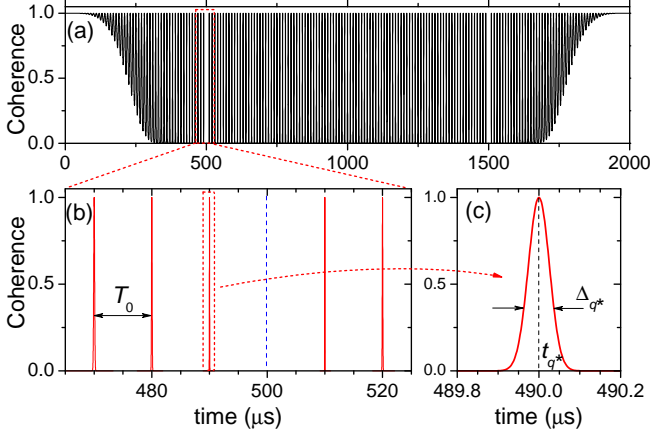


FIG. 2. (Color online) (a) The time-comb structure of qubit coherence under 100-pulse CPMG control. For $\omega_0 t \gg 1$, the comb period is synchronized with the oscillator period $T_0 = 2\pi/\omega_0$. (b) Close-up of the coherence peaks. A missing peak at $\omega_0 t = N\pi$ is indicated by the blue dashed line. The peak width is decreasing when getting close to the missing one. (c) Close-up of the narrowest coherence peak, which is centered at t_{q^*} with width Δ_{q^*} (see text). The parameters used in this figure are oscillator frequency $\omega_0/(2\pi) = 100$ kHz, coupling strength $\lambda = 0.001\omega_0$, temperature $T = 10$ K and 100-pulse CPMG control.

quality factor up to 10^{10} [25] or even higher, which enables such systems to detect novel quantum effect [26–28]. Here, we combine the advanced qubit and opomechanical systems, and propose that hybrid systems such as optically levitated nano-diamond with a single NV center [29–31] can realize a high mass sensitivity up to of 10^{-22} g/ $\sqrt{\text{Hz}}$ in room temperature.

Time-comb under dynamical decoupling. We consider a coupled qubit-oscillator model with the Hamiltonian [30–32]

$$H = \frac{1}{2}\omega_q\sigma_z + \omega_0 b^\dagger b + \frac{1}{2}\lambda\sigma_z(b^\dagger + b), \quad (1)$$

where ω_0 (ω_q) is the frequency of the harmonic oscillator (qubit), and λ is the coupling strength. The qubit is initially prepared in a superposition state $|\psi(0)\rangle_q = (|0\rangle + |1\rangle)/\sqrt{2}$. The oscillator is initially in a thermal equilibrium state $\rho_b = Z^{-1} \exp(-\beta\omega_0 b^\dagger b)$ with the partition function $Z = \text{Tr}[\exp(-\beta\omega_0 b^\dagger b)]$ and the inverse environmental temperature $\beta = 1/(k_B T)$.

Since σ_z is a good quantum number in Eq. (1), we focus on the dynamics of the relative phase, or quantum coherence [33], between qubit states $|0\rangle$ and $|1\rangle$ influenced by the oscillator. Under DD control of the qubit, which flips the qubit state by a train of π pulses applied at times t_j for $j = 1, 2, \dots, N$ (with $t_0 \equiv 0$ and $t_{N+1} \equiv t$), the qubit coherence $L(t)$ is expressed as [34]

$$L(t) = \langle \mathcal{T}_c e^{-i \int_c \hat{X}(t') f(t') dt'} \rangle, \quad (2)$$

where the integral is performed on a time contour $c : 0 \rightarrow t \rightarrow 0$, \mathcal{T}_c is the contour-time-ordering operator, and $\hat{X}(t) =$

$\lambda(b^\dagger e^{i\omega_0 t} + b e^{i\omega_0 t})$ is proportional to the oscillator displacement in the interaction picture. The qubit flipping by DD control is described by the sign function $f(t)$, which toggles between $+1$ or -1 whenever a π -pulse is applied.

The Gaussian statistics nature of the harmonic oscillator allows the coherence in Eq. (2) to be exactly evaluated [32, 35]. Particularly, under the N -pulse CPMG sequence [with N qubit flips at $t_j = (2j - 1)/(2N)$], the qubit coherence is $L(t) = \exp[-\chi(t)/2]$ with [32, 35]

$$\begin{aligned} \chi(t) &= \int_0^\infty \frac{d\omega}{\pi} S(\omega) |F(\omega t)|^2 = \frac{4\tilde{\lambda}^2}{\omega_0^2} \left(\sec \frac{\omega_0 t}{2N} - 1 \right)^2 \sin^2 \frac{\omega_0 t}{2} \\ &\equiv \Gamma^2(t) \sin^2 \frac{\omega_0 t}{2}, \end{aligned} \quad (3)$$

where $S(\omega) = \tilde{\lambda}^2 \pi \delta(\omega - \omega_0)$ is the noise spectrum of the oscillator, $F(\omega t)$ is the Fourier transform of the modulation function $f(t)$, $\tilde{\lambda}^2 = \lambda^2(2n_{\text{th}} + 1)$, and $n_{\text{th}} \equiv [\exp(\beta\omega_0) - 1]^{-1}$ is the thermal occupation number of the oscillator. In the second line of Eq (3), $\Gamma(t)$ is a slow-varying envelope function.

The qubit coherence exhibits novel dynamics with many-pulse ($N \gg 1$) DD, as shown in Fig. 2. In short time limit ($\omega_0 t \ll N\pi$), the qubit coherence is well-protected (close to unity) by the DD control. As increasing time t , the qubit coherence become oscillating. Furthermore, when $\Gamma(t) \gg 1$, the qubit enters a new regime where the coherence almost decays completely [$L(t) \approx 0$], *except* in the narrow intervals around the zero points of Eq. (3), i.e., $t_q = qT_0$ [for integer q and $q \neq (2k + 1)N/2$], where $T_0 = 2\pi/\omega_0$ is the oscillator period. In this regime, the qubit coherence forms a *comb structure*.

In the time-comb regime, the coherence shows sharp peaks in Gaussian shapes $L(t) \approx e^{-\gamma_q^2(t-t_q)^2/2}$ [see. Fig. 2(c)]. The peak width decreases when t_q approaches odd-multiple of $N\pi/\omega_0$ [i.e. the diverge point of $\Gamma(t)$, indicated by the blue dashed line in Fig. 2(b)]. For a given control pulse number N , the narrowest peak (for $q = q^* \equiv N/2 - 1$) appears at t_{q^*} and with peak width Δ_{q^*}

$$\begin{aligned} t_{q^*} &= \left(\frac{N}{2} - 1 \right) T_0, \\ \Delta_{q^*} &\equiv \frac{2\sqrt{2}}{\gamma_{q^*}} = \frac{T_0}{N\Lambda\sqrt{2n_{\text{th}} + 1}}, \end{aligned} \quad (4)$$

where $\Lambda = \lambda/\omega_0$ is the ratio of the coupling strength to the oscillator frequency. Notice that peak width is *inversely proportional* to the control pulse number N and the square root of the thermal excitation number n_{th} (for $n_{\text{th}} \gg 1$). In the following, we will show that the peak narrowing with increasing N or n_{th} (i.e., increasing temperature T) improves the sensitivity.

Ultra-sensitive mass spectrometer. We propose that the time-comb can be used to measure tiny mass change of the mechanical oscillator, e.g. due to absorption of single molecules, by monitoring shifts of the qubit coherence peaks. For an oscillator with oscillation frequency $\omega_0 = \sqrt{k/M}$ (for k and M being the spring constant and the mass, respectively), a small change δM of the mass M induces a change δL of the

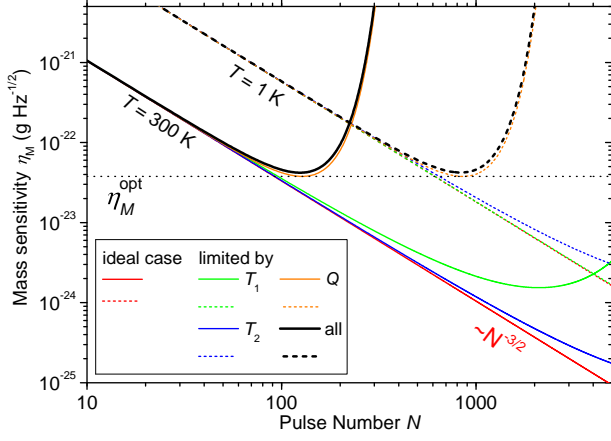


FIG. 3. (Color online) Mass sensitivity η_M as functions of DD control pulse number N . Solid curves are the sensitivity in room temperature $T = 300$ K, while dashed curves are the sensitivity in low temperature $T = 1$ K. The red curves are the ideal sensitivity according to Eq. (6), which scales as $\sim N^{-3/2}$. The curves in green, blue, and orange are the sensitivity taking into account the qubit T_1 -decay (with $T_1 = 7$ ms), qubit T_2 -decay (with $T_2 = 100$ μ s), and oscillator finite Q -factor (with $Q = 10^9$), in turn. The thick black curves are the sensitivity with all the decay mechanisms included. The horizontal dotted line indicates the temperature-independent optimal sensitivity. Other parameters (ω_0 and λ) used in this figure are the same as those in Fig. 2.

coherence $L(t)$ around the recovery peak. The relative mass uncertainty is

$$\frac{\delta M}{M} = \frac{2\delta\omega_0}{\omega_0} = \frac{1}{\gamma_{q^*}^2(t - t_{q^*})t_{q^*}} \frac{\delta L}{L} \approx \frac{1}{\gamma_{q^*}t_{q^*}} \frac{\delta L}{L}, \quad (5)$$

where we have chosen a proper measurement time t close to the peak time t_{q^*} so that $\gamma_{q^*}(t - t_{q^*}) \approx 1$.

We consider the case where the qubit coherence is obtained by averaging the output of N_{run} independent Bernoulli trials. In this case, the uncertainty δL comes from the shot-noise in the measurement, i.e. $\delta L/L \approx N_{\text{run}}^{-1/2}$. For the total measurement time $T_{\text{tot}} = N_{\text{run}}t_{q^*}$, the mass sensitivity η_M , up to a constant of the order of unity, is

$$\eta_M \equiv \delta M \sqrt{T_{\text{tot}}} = \frac{M}{(2N)^{3/2} \Lambda \sqrt{k_B T / \hbar}}, \quad (6)$$

where \hbar is Planck constant. Here we have assumed that $N \gg 1$ and $n_{\text{th}} \approx k_B T / \hbar \omega_0 \gg 1$, which is the case for most practical mechanical oscillator systems.

Equation (6) reveals two interesting features of the qubit-oscillator based mass spectrometer. Firstly, the scaling relation of sensitivity to the pulse number N is different with that appears in magnetometry. In the case of using qubit for magnetometry under DD, the sensitivity scales with the control pulse number as $\sim N^{-1/2}$ [13]. In our case, the narrowing effect of the peak when increasing the pulse number N improves the scaling relation to $\sim N^{-3/2}$, which will help to achieve the optimal sensitivity faster.

Secondly, and more interestingly, the sensitivity is *inverse-linearly* dependent on the square root of temperature. For the conventional oscillator-based sensor, the sensitivity is usually limited by thermal fluctuation of the oscillator displacement x , which is characterized by the root-mean-square amplitude $x_{\text{rms}} = \sqrt{k_B T / k}$. High temperature would destroy the sensitivity, and prevent the room-temperature applications. While in our measurement scheme, the measured quantity ω_0 does not directly couple to the oscillator displacement x and, thus, its uncertainty is independent on the position thermal fluctuation. Instead, the more thermal phonons in higher temperature cause stronger effective coupling between the qubit and oscillator, which improves the sensitivity.

Sensitivity limitations.— Now we analyse the factors which limit the ideal sensitivity shown in Eq. (6). The qubit decoherence (including relaxation and dephasing) and the oscillation dissipation caused by the inevitable coupling to the environment are the two reasons which set lower bound to the sensitivity.

The environmental fluctuation to the qubit, which causes the qubit decoherence, prevents the perfect recovery of coherence shown in Fig. 2. With both longitudinal relaxation process (or T_1 -process) and transverse relaxation process (or T_2 -process), the qubit suffers a background decoherence $L_{\text{bg}}(t)$ in addition to the oscillator-induced periodic revival peaks. Taking the solid state spin qubit for example, the background decoherence can be modelled as $L_{\text{bg}}(t) = \exp[-t/T_1 - (t/T_2^{(N)})^3]$ [36]. The longitudinal decoherence, typically caused by phonon scattering, is a Markovian process (a simple exponential decay), and is hardly corrected by DD. The transverse decoherence, usually caused by spin baths, can be protected by DD with the decay time $T_2^{(N)}$ depending on the DD control pulse number N as $T_2^{(N)} = T_2 N^{2/3}$ [36] (for T_2 being the coherence time for $N = 1$).

The background qubit decoherence $L_{\text{bg}}(t)$ reduces the height of the recover peaks. Consequently, the mass sensitivity is magnified by a factor of $L_{\text{bg}}^{-1}(t_{q^*})$. The balance between the $\sim N^{-3/2}$ sensitivity scaling and the background decoherence gives rise to an optimal pulse number to the sensitivity (see Fig. 3), similar to Ref. [13] but with an additional peak narrowing effect. Qubit with long coherence time, like NV centers in diamond, can be chosen to eliminate the background decoherence $L_{\text{bg}}(t)$ effect. In low temperature, the T_1 time can reach the order of seconds [37], and the T_2 time has been demonstrated to be \sim ms or even longer under DD control [38]. In this case, the qubit decoherence becomes less important, and the dissipation of mechanical oscillation is the dominant mechanism limiting the sensitivity.

The coupling to the environment of mechanical resonator causes broadening of the oscillator frequency. In Eq. (3), with the δ -function in the noise spectrum $S(\omega)$ replaced by a Lorentzian spectrum with finite broadening $\kappa = \omega_0/Q$ [i.e. $S(\omega) = \lambda^2 \kappa / [(\omega - \omega_0)^2 + \kappa^2]$, for Q being the quality factor], the coherence cannot recover perfectly even though the central oscillation frequency hits the zero points of the filter

function. The overlap between the wings of the Lorentzian spectrum and the non-zero region of the function $F(\omega t)$ causes the reduction of the height of the coherence recovery peak [see Eq. (3)]. In the case of $Q \gg N \gg 1$, the function $\chi(t)$ around the recovery time $t = t_{q^*}$ is calculated as $\chi(t) \approx \chi(t_{q^*}) + \gamma_{q^*}^2(t - t_{q^*})^2$ with $\chi(t_{q^*}) = 4\tilde{\lambda}^2 N^3 / (\omega_0^2 Q)$. Increasing the pulse number N reduces the recovery height. The optimal control pulse number N_{opt} is estimated by $\chi(t_{q^*}) \approx 1$, which gives

$$N_{\text{opt}} \approx \frac{\omega_0}{2\lambda} \left(\frac{\hbar \lambda Q}{k_B T} \right)^{\frac{1}{3}}. \quad (7)$$

Substitute the optimal pulse number N_{opt} into Eq. (6), one obtains a universal value of the optimal mass sensitivity (up to a constant of the order of unity)

$$\eta_M^{\text{opt}} = \frac{M}{\sqrt{f_0 Q}}, \quad (8)$$

where $f_0 = \omega_0/(2\pi)$. In this case, the optimal sensitivity only relies on the properties of the oscillator (i.e., f_0 and Q), and is *independent* on the temperature T nor the qubit-oscillator coupling strength λ . In addition to the temperature-independent feature, we notice that in higher temperature, less controlled pulses are required to reach the optimal sensitivity according to Eq. (7) (see Fig. 3). In this sense, the proposed mass spectrometer has better performance in high temperature, in sharp contrast to conventional schemes that low temperature is necessary to reduce the thermal fluctuation. The universal form of the optimal sensitivity in Eq. (8) provides a simple guiding principle to design the system and to experimentally implement our proposal. The model and the sensitivity described in Eqs. (1)-(8), indeed, is quite general, and can be realized in different types of system. In the following, we take the optically levitated nano-diamond with NV center as an example to demonstrate the application.

Experimental feasibility.- As we discussed above, solid state spin with long coherence time, like nitrogen-vacancy in diamond, serves as a good candidate of the qubit. The T_1 and T_2 decoherence has negligible effect in the sensitivity (see Fig. 3). Meanwhile, the coherent coupling between NV center electron spin and the mechanical motion has been demonstrated very recently [32] with a low- Q mechanical cantilever. Since high quality factor Q of the mechanical oscillator is essential for the ultimate sensitivity, we propose that the system of optically levitated nano-diamond with a single NV center is a good candidate for realizing the ultra-sensitive mass spectrometer, where the quality factor can reach $\sim 10^{10}$ or even higher.

Consider a nano-diamond of 50 nm in diameter (corresponding to the mass $M = 2.3 \times 10^{-16}$ g) which is optically trapped in a harmonic potential with center-of-mass (CoM) oscillating frequency $f_0 = 100$ kHz. In a gradient magnetic field, the CoM motion of the nano-diamond couples to the NV center electron spin in the nano-diamond in a manner described in Eq. (1). With the magnetic field gradient

$G_m = 200$ T/m, the coupling strength is ~ 100 Hz. With the quality factor $Q = 10^9$, the system can reach a mass sensitivity of the order $\sim 10^{-22}$ g/ $\sqrt{\text{Hz}}$. In practical experiments, the efficiency of the optical readout of the spin state of NV center is limited by the spin-selective fluorescence contrast, and the photon collection efficiency. This gives rise to a technique factor $1/C \approx 10^{-2} \sim 10^{-1}$ unfavourable for the sensitivity [39]. However, even though the technique factor may deteriorate the sensitivity by one or two orders of magnitudes, the temperature-independent feature of our proposed system will be still attractive for a room temperature sensor.

Conclusion.- In this paper, we propose an ultra-sensitive mass spectrometer based on the coupled qubit-oscillator system. Using the many-pulse DD technique, the qubit coherence exhibits a time-comb structure, which enable the precise measurement of the oscillating frequency. The combination of advanced techniques on NV center in diamond and optical levitated nano-particle, which serve as long-live qubit and high quality oscillator respectively, makes the room-temperature ultra-sensitive mass spectrometer ready to be realized.

We thank Dr. L. Ge, Professor Y. Li, Professor W. Yang, Professor C.P. Sun, and Professor J. Twamley for fruitful discussion about theoretical scheme, and Dr. T.C. Li, Dr. F. Xue, Dr. Y. Tao for suggestions on the experimental feasibility. N.Z. is supported by NSFC No. 11374032. Z.Q.Y. is funded by the NBRPC (973 Program) 2011CBA00300 (2011CBA00302), NNSFC 11105136, and 61033001.

* nzhao@csrc.ac.cn; <http://www.csrc.ac.cn/~nzhao>

- [1] N. Zhao, S.-w. Ho, and R.-b. Liu, *Physical Review B* **85**, 115303 (2012).
- [2] S. Kolkowitz, Q. P. Unterreithmeier, S. D. Bennett, and M. D. Lukin, *Physical Review Letters* **109**, 137601 (2012).
- [3] T. H. Taminiau, J. J. T. Wagenaar, T. van der Sar, F. Jelezko, V. V. Dobrovitski, and R. Hanson, *Physical Review Letters* **109**, 137602 (2012).
- [4] H. J. Mamin, M. Kim, M. H. Sherwood, C. T. Rettner, K. Ohno, D. D. Awschalom, and D. Rugar, *Science (New York, N.Y.)* **339**, 557 (2013).
- [5] T. Staudacher, F. Shi, S. Pezzagna, J. Meijer, J. Du, C. a. Meriles, F. Reinhard, and J. Wrachtrup, *Science (New York, N.Y.)* **339**, 561 (2013).
- [6] J.-J. Li and K.-D. Zhu, *Physics Reports* **525**, 223 (2013).
- [7] M. Ganzhorn, S. Klyatskaya, M. Ruben, and W. Wernsdorfer, *Nature nanotechnology* **8**, 165 (2013).
- [8] J. Chaste, a. Eichler, J. Moser, G. Ceballos, R. Rurali, and a. Bachtold, *Nature nanotechnology* **7**, 301 (2012).
- [9] K. Jensen, K. Kim, and a. Zettl, *Nature nanotechnology* **3**, 533 (2008).
- [10] A. K. Naik, M. S. Hanay, W. K. Hiebert, X. L. Feng, and M. L. Roukes, *Nature Nanotechnology* **4**, 445 (2009).
- [11] D. Rugar, R. Budakian, H. J. Mamin, and B. W. Chui, *Nature* **430**, 329 (2004).
- [12] L. Viola, E. Knill, and S. Lloyd, *Physical Review Letters* **82**, 2417 (1999).
- [13] G. de Lange, D. Ristè, V. V. Dobrovitski, and R. Hanson, *Physical Review Letters* **106**, 080802 (2011).

- [14] J. Sidles, J. Garbini, K. Bruland, D. Rugar, O. Züger, S. Hoen, and C. Yannoni, *Reviews of Modern Physics* **67**, 249 (1995).
- [15] A. Gruber, A. Drabenstedt, C. Tietz, L. Fleury, J. Wrachtrup, and C. von Borczyskowski, *Science* **276**, 2012 (1997).
- [16] J. Wrachtrup and F. Jelezko, *Journal of Physics-condensed Matter* **18**, S807 (2006).
- [17] G. Balasubramanian, P. Neumann, D. Twitchen, M. Markham, R. Kolesov, N. Mizuochi, J. Isoya, J. Achard, J. Beck, J. Tissler, V. Jacques, P. R. Hemmer, F. Jelezko, and J. Wrachtrup, *Nature Materials* **8**, 383 (2009).
- [18] A. N. Cleland, *Foundations of Nanomechanics: From Solid-State Theory to Device Applications* (Springer, 2003).
- [19] F. Marquardt and S. Girvin, *Physics* **2**, 40 (2009).
- [20] M. Aspelmeyer, T. J. Kippenberg, and F. Marquardt, *arXiv* (2013), *arXiv:1303.0733v1*.
- [21] O. Romero-Isart, M. L. Juan, R. Quidant, and J. I. Cirac, *New Journal of Physics* **12**, 033015 (2010).
- [22] D. E. Chang, C. a. Regal, S. B. Papp, D. J. Wilson, J. Ye, O. Painter, H. J. Kimble, and P. Zoller, *Proceedings of the National Academy of Sciences of the United States of America* **107**, 1005 (2010).
- [23] T. Li, S. Kheifets, D. Medellin, and M. G. Raizen, *Science* **328**, 1673 (2010).
- [24] T. Li, S. Kheifets, and M. G. Raizen, *Nature Physics* **7**, 527 (2011).
- [25] Z.-Q. Yin, A. a. Geraci, and T. Li, *International Journal of Modern Physics B* **27**, 1330018 (2013).
- [26] A. a. Geraci, S. B. Papp, and J. Kitching, *Physical Review Letters* **105**, 101101 (2010).
- [27] A. Arvanitaki and A. a. Geraci, *Physical Review Letters* **110**, 071105 (2013).
- [28] Z.-Q. Yin, T. Li, and M. Feng, *Physical Review A* **83**, 013816 (2011).
- [29] L. P. Neukirch, J. Gieseler, R. Quidant, L. Novotny, and A. Nick Vamivakas, *Optics Letters* **38**, 2976 (2013).
- [30] M. Scala, M. S. Kim, G. W. Morley, P. F. Barker, and S. Bose, *Physical Review Letters* **111**, 180403 (2013).
- [31] Z.-Q. Yin, T. Li, X. Zhang, and L. M. Duan, *Physical Review A* **88**, 033614 (2013).
- [32] S. Kolkowitz, a. C. Bleszynski Jayich, Q. Unterreithmeier, S. D. Bennett, P. Rabl, J. G. E. Harris, and M. D. Lukin, *Science* **335**, 1603 (2012).
- [33] W. Yang, Z.-Y. Wang, and R.-B. Liu, *Frontiers of Physics in China* **6**, 1 (2010).
- [34] W. Yang and R.-B. Liu, *Physical Review B* **78**, 085315 (2008).
- [35] N. Zhao, J. Hu, S. Ho, J. Wan, and R. Liu, *Nature nanotechnology* **6**, 242 (2011).
- [36] G. de Lange, Z. H. Wang, D. Riste, V. V. Dobrovitski, and R. Hanson, *Science* **330**, 60 (2010).
- [37] S. Takahashi, R. Hanson, J. van Tol, M. S. Sherwin, and D. D. Awschalom, *Physical Review Letters* **101**, 47601 (2008).
- [38] N. Bar-Gill, L. M. Pham, C. Belthangady, D. Le Sage, P. Cappellaro, J. R. Maze, M. D. Lukin, A. Yacoby, and R. Walsworth, *Nature communications* **3**, 858 (2012), *arXiv:1112.0667*.
- [39] J. M. Taylor, P. Cappellaro, L. Childress, L. Jiang, D. Budker, P. R. Hemmer, A. Yacoby, R. Walsworth, and M. D. Lukin, *Nature Physics* **4**, 810 (2008).